RSC Advances

PAPER

View Article Online
View Journal | View Issue

Cite this: *RSC Adv.*, 2025, **15**, 49643

Functional nano-nucleic acid platform promotes copper-induced gastric cancer cell death

Hao Zhang,†[a] Bing Ding†[b] and Qingyan Kou *[c]

Received 10th October 2025
Accepted 4th December 2025

DOI: 10.1039/d5ra07735d

rsc.li/rsc-advances

The targeted design of nanomedicine has revolutionized tumor therapy. We report an all-in-one ZnO@DNAzyme-Cu(II)Elesclomol nanoplatform that synchronously silences ATP7B and escorts Cu^{2+} to evoke cuproptosis. The DNAzyme within the nanoparticle was independently designed to target ATP7B, a key regulator of cuproptosis. This multifunctional nanoplatform can be efficiently internalized by gastric cancer cells (SGC7901), where it undergoes degradation and releases its active components. ZnO NPs act as a reservoir for zinc ions, which facilitate the catalytic activity of DNAzyme, enabling it to target and suppress ATP7B mRNA expression. Additionally, ZnO NPs reduce intracellular glutathione (GSH) levels, enhance reactive oxygen species (ROS) production, and elevate oxidative stress in tumor cells. The subsequent release of Cu(II)-Elesclomol triggers copper-induced cell death. Both *in vitro* and *in vivo* experiments demonstrated that this nanoplatform effectively inhibits tumor progression and promotes tumor cell death. This proposed nanoplatform holds significant promise for multifunctional cancer therapy and personalized nanomedicine.

Introduction

Copper ions, as essential trace elements, play a crucial role in cellular physiological processes.[1,2] The intracellular concentration of copper is typically low and tightly regulated; disruption of copper homeostasis can lead to cell death and severe diseases such as Menkes disease,[3] Wilson's disease,[4] amyotrophic lateral sclerosis.[5] Recently, researchers have identified a novel form of cell death dependent on copper ions, termed "cuproptosis".[6] Exploring the cytotoxic response triggered by intracellular copper accumulation is a key step in developing new therapeutic strategies. Cuproptosis is a unique mode of cell death induced by excessive accumulation of Cu^{2+}, distinguishing it from other forms of cell death such as apoptosis, pyroptosis, and ferroptosis. Intracellular copper binds specifically to acylated components of the tricarboxylic acid (TCA) cycle, leading to the aggregation of acylated mitochondrial proteins. This aggregation subsequently results in the depletion of Fe–S clusters, inducing proteotoxic stress and ultimately causing cell death. Several key regulators of cuproptosis have been identified: FDX1, a critical Fe–S cluster protein, reduces Cu^{2+} to Cu^{1+} and promotes copper accumulation;[7] LIAS catalyzes protein acylation, and its high expression enhances cuproptosis;[8] ATP7A/ATP7B regulate intracellular copper homeostasis by controlling copper uptake and efflux.[9]

A large number of studies have focused on the applications of nanomaterials in cuproptosis. One study coated a hybrid membrane derived from M2 macrophages and osteogenically induced human bone marrow mesenchymal stem cells onto Mn/Ca dual-atom nanozymes. These nanozymes were found to inhibit cuproptosis, promote mucosal healing, and increase bone volume fraction.[10] A nanozyme self-assembled from copper ions and ellagic acid was shown to enhance cuproptosis under near-infrared irradiation and accelerate tissue repair.[11] A glucose oxidase-modified copper–apigenin network nanoshuttle was able to promote cuproptosis and demonstrated strong therapeutic efficacy in an ovarian tumor model.[12]

DNAzymes are synthetic single-stranded deoxyribonucleic acids with catalytic activity.[13] Due to their programmability, stability, and simplicity, DNAzymes have attracted significant attention in therapeutic, diagnostic, and biosensing applications. DNAzymes are typically designed to cleave specific mRNA sequences, thereby downregulating gene expression. The two most commonly used DNAzyme sequences are 8–17 DNAzyme and 10–23 DNAzyme. The 8–17 DNAzyme consists of a three-base-pair stem, an AGC trinucleotide loop, and a WCGR(A) loop (where W = A/T and R = A/G).[14] The 10–23 DNAzyme, one of the most widely studied RNA-cleaving DNAzymes, consists of a 15-nucleotide catalytic loop flanked by two hybridization arms.[15] The length and sequence of these arms can be varied to

[a]*Department of Gastrointestinal Surgery, Xiangan Hospital of Xiamen University, School of Medicine, Xiamen University, Xiamen, 361000, China. E-mail: 1069038786@qq.com*

[b]*Department of Anesthesiology, Qingdao Traditional Chinese Medicine Hospital, Qingdao Hiser Hospital Affiliated of Qingdao University, 266000, China. E-mail: dingbing0510@126.com*

[c]*Department of General Surgery, Qingdao Central Hospital, University of Health and Rehabilitation Sciences, Qingdao, 266000, China. E-mail: 279708830@qq.com*

† These authors contributed equally.

target almost any RNA of interest. DNAzyme activity requires high concentrations of metal ions, which are often insufficient in normal cellular environments. Furthermore, DNAzymes are susceptible to degradation by nucleases before reaching target cells, posing a challenge for their therapeutic application. ZnO serves both as a protective carrier and an *in situ* Zn^{2+} reservoir to meet the catalytic demands of 10–23 DNAzymes.

With advancements in nanomaterials research, researchers have discovered that nanoparticles can be readily internalized by cells. Consequently, many researchers have utilized metal nanoparticles to deliver DNAzymes into cells, protecting them from degradation and enhancing their therapeutic potential. Various DNAzyme-nanoparticle conjugates have been synthesized, demonstrating promising applications in disease treatment. It has been reported that ZnO NPs and DNAzyme combined with the platinum(IV) prodrug can effectively treat multi-drug resistant tumors.[16] Developing a degradable biomimetic DNAzyme biocapsule for high-efficiency gene therapy of both primary and pulmonary metastatic breast tumors.[17]

At present, apart from surgical resection, there is no better way to treat gastric cancer. The development of nanotechnology has provided a new treatment approach. For the first time, DNAzyme for ATP7B was proposed in our study. ZnO NPs were used to adsorb DNAzymes, forming a carrier platform that not only protects DNAzymes from degradation but also facilitates intracellular delivery of Cu(II)-Elesclomol. This approach effectively induces copper-dependent tumor cell death, providing new insights into cancer therapy (Scheme 1).

Materials and methods

Materials and reagents

ZnO was purchased from Aladdin (Shanghai, China). Cu(II)-Elesclomol(ES) was purchased from MedChemExpress (MCE, Shanghai). Antibodies for western blot analysis contains ATP7B (from Abcam, USA), HMOX1(from Proteintech, China), GPX4(from Proteintech, China), DLAT (from Proteintech, China), FDX1(from Proteintech, China), GAPDH (from ABclonal, China). Reactive oxygen species assay Kit was sourced from Beyotime (Shanghai, China). Low molecular weight protein (Marker, 10–180 kDa), were brought from Shanghai Yuanye Biotechnology Co., Ltd (Shanghai, China). The RIPA, protease inhibitor cocktail, BCA Protein Assay Kit, 5X loading buffer was sourced from Solarbio (Beijing, China). All oligonucleotides were synthesized by Sangon Biotechnology Co., Ltd (Shanghai, China), and their sequences are listed in Table 1.

Preparation of ZnO@DE

Weigh ZnO nanoparticles (10 mg ml^{-1}, 10 ml), Cu(II)-Elesclomol (1 mg ml^{-1}, 7 ml) and mix with the DNAzyme solution (100 μM, 5 ml) to achieve ZnO@DNAzyme. Stir for 12 hours, centrifuge, and wash with ethanol three times. Dry the nanomaterials in a vacuum oven at 40 °C.

Characterization

The surface morphology of nanoparticles was observed using the Hitachi HT7700 microscope (Hitachi, Japan).[16] Elemental analysis was conducted *via* X-ray diffraction (Xtalab Synergy,

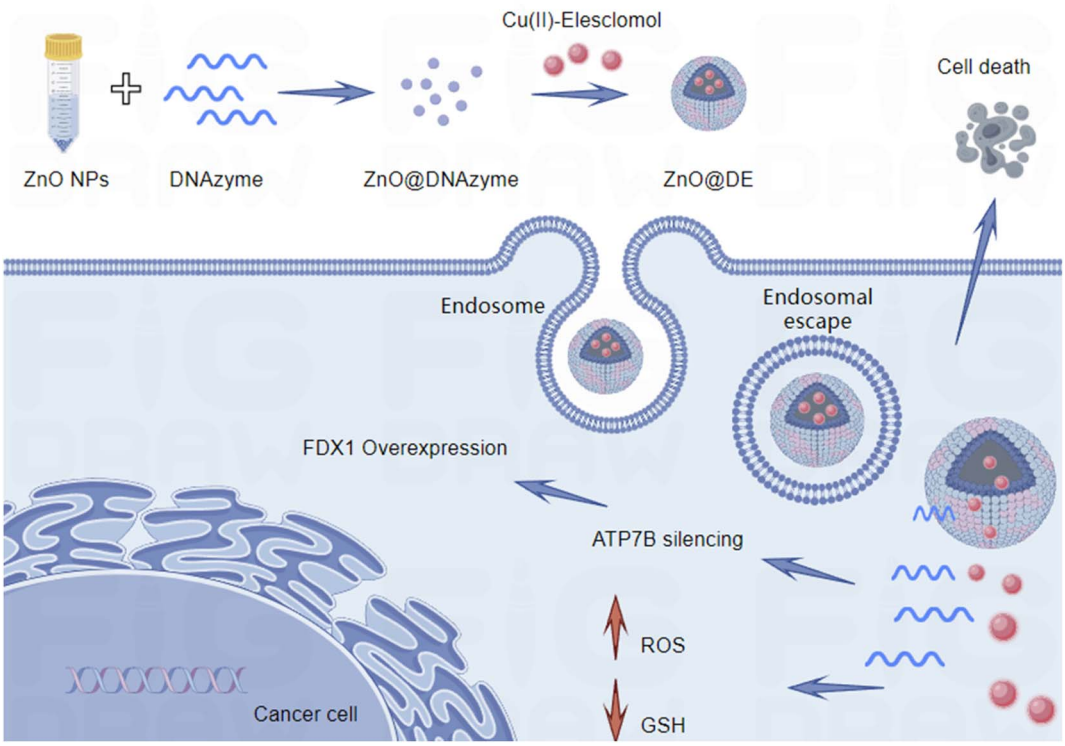

Scheme 1 Schematic diagram of the synthesis process of ZnO@DE and the mechanism.

Table 1 Sequence of oligonucleotides used in this study

Names	Sequence (5′ → 3′)
DNAzyme[1]	TTTATCTTGTAGGCTAGCTACAACGAGCGCCATCTCC
DNAzyme[2]	CTTTCTCTTGAGGCTAGCTACAACGATGCGCCATGTCC
DNAzyme[3]	TTTATCTTGTAGGCTAGCTACAACGAGCGCCATCTCCA
DNAzyme(M)	TTTATCTTGTATCGCTCCAAATAGTGAGTCGCTC
ATP7B forward primer	GGAGATGGCGCACAAGATAA
ATP7B reverse primer	CACAGCCAGAACCTTCCTGA

Netherlands). Dynamic light scattering (DLS) was carried out in suspensions using the zeta potentiometer (Zetasizer Nano ZS, England). X-ray photoelectron spectroscopy (XPS) analysis was performed using the ESCALAB 250 (Thermo, USA).

Cell culture

Cells were cultured at 37 °C in a 5% CO2 incubator. All media were supplemented with 10% fetal bovine serum (Gibco, USA), 50 μg ml^{-1} penicillin, and 50 μg ml^{-1} streptomycin (Gibco, USA). Cell lines SGC7901 and MC38 (from National Collection of Authenticated Cell Cultures, Shanghai) was maintained in 1640 medium (Gibco, USA). Observe the morphology and growth status of cells under a common optical microscope.

Cytotoxicity assay

Cell viability was assessed using the CCK-8 assay (MCE, Shanghai, China) with different nanoparticle concentrations. After 24 hours, 10 μl CCK-8 reagent was added, and absorbance at 450 nm was measured.

Cytotoxicity assay

For hemolysis testing, fresh mouse blood was collected and mixed with anticoagulant and saline to assess the hemolytic potential of nanoparticles. Blood diluted with distilled water served as a positive control. Samples were incubated at 37 °C for 4 hours, centrifuged at 2500 rpm for 10 minutes, and the absorbance of the supernatant was recorded at 545 nm using a microplate reader.

Determination of intracellular ROS

Cells were evenly seeded in a 6-well plate in equal amounts and divided into six groups. When the cell density reached approximately 75%, the culture medium was replaced, and different nanoparticles were added to each group. After 2 hours of incubation, the cell culture medium was removed, and 1 ml of pre-diluted detection solution (Beyotime, Shanghai) was added to each well. The plate was incubated at 37 °C in a cell incubator for 20 minutes. Cells were then washed three times with PBS. The ROS fluorescence signal intensity of each group was observed under a fluorescence microscope.

Real-time PCR

Total RNA was extracted using the RNA-Easy Kit (Vazyme, Nanjing, China). RNA was then reverse-transcribed into cDNA using the PrimeScript™ RT reagent Kit with gDNA Eraser (Takara). RT-qPCR was performed using TB Green® Premix Ex Taq™ II (Takara). The primer sequences are shown in Table 1.

Western blot

The cells were treated after 24-hours nanoparticle. Total protein was extracted using RIPA buffer. Proteins were separated on 10% SDS-PAGE and transferred to PVDF membranes. Membranes were blocked with 5% nonfat milk for 1.5 hours at 24 °C, incubated with primary antibodies overnight in 4 °C, and with HRP-conjugated secondary antibodies for 1–2 hours. Protein levels were detected using ECL reagents.

Animal experiments

All animal procedures were performed in accordance with the Guidelines for Care and Use of Laboratory Animals of Xiamen University and approved by the Animal Ethics Committee of Xiamen University. C57BL/6J mice were randomly divided into groups and injected subcutaneously with MC38 cells. Treatments were administered on the day of cell implantation, and tumor growth was monitored every three days for two weeks.

Statistical analysis

The data analyses were carried out using GraphPad Prism8. Data were analyzed using *t*-tests for two-group comparisons and one-way ANOVA for multiple groups. Wilcoxon and Kruskal–Wallis tests were used for non-normally distributed data. Statistical significance was defined as $p < 0.05$ ($p < 0.01$ for highly significant).

Results and discussion

Characterization of ZnO@DE

The synthesis process of the functional nucleic acid nanoplatform ZnO@DE first involves the formation of ZnO@DNAzyme by synthesizing ZnO with DNAzyme, followed by mixing ZnO@DNAzyme with Cu(II)-Elesclomol (ES) to form ZnO@DE. The transmission electron microscopy (TEM) image of this nanoparticle is shown in Fig. 1A and 1B, presents the size distribution of the nanoparticles. ZnO@DNAzyme aggregates due to the adsorption of a large amount of DNA by ZnO, resulting in an increased particle size, which is predominantly around 200 nm. With the addition of ES to ZnO@DNAzyme, the particle size of ZnO@DE increased to approximately 250 nm. Additionally, we measured the zeta potential of ZnO@DE (Fig. 1C). ZnO exhibits a positive potential, whereas ES and nucleic acids exhibit negative potentials. The nanoplatform was further analyzed using X-ray diffraction (XRD) and X-ray photoelectron spectroscopy (XPS) (Fig. 1D and E). The XRD results show that the main peaks are located at 31.78°, 34.38°, 36.2°, 47.58°, 56.62°, 62.98°, 68.04° and 69.12°and their planes are (1 0 0), (0 0 2), (1 0 1), (1 0 2), (1 1 0), (2 0 0), (1 1 2), and (2 0 1).

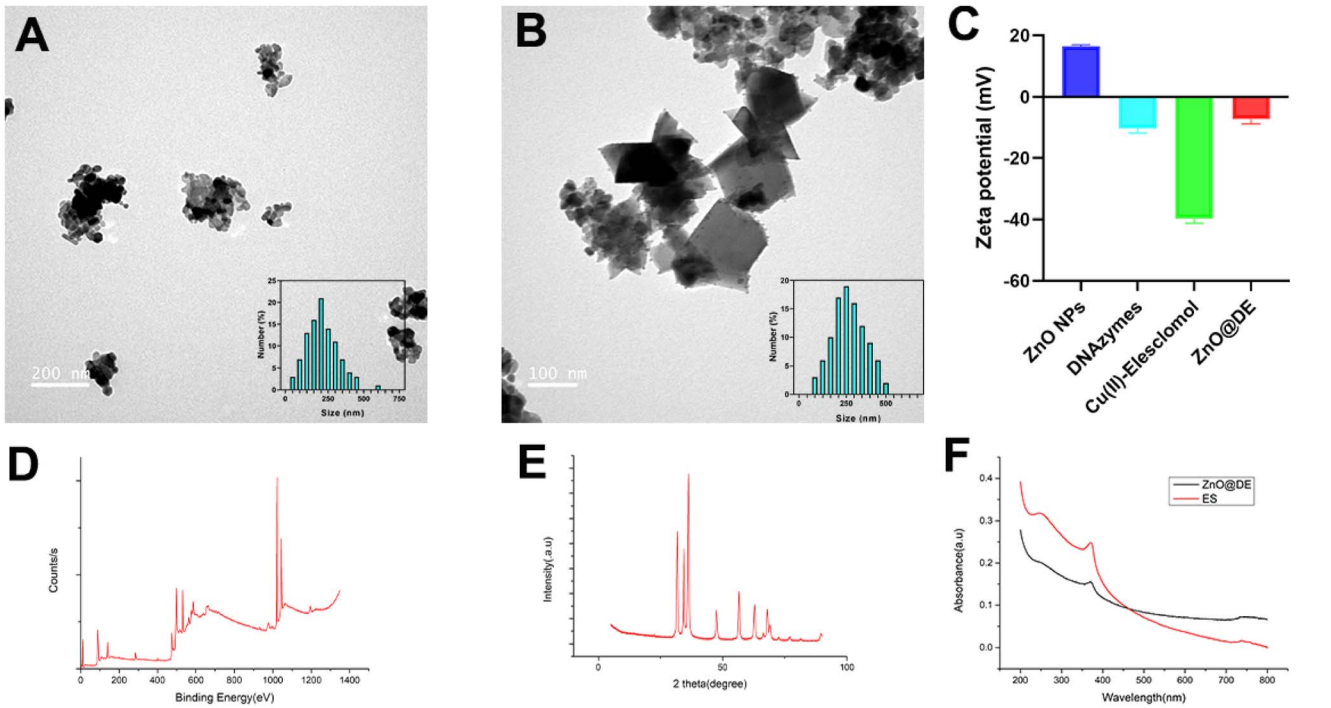

Fig. 1 Characterization of ZnO@DE. (A and B) TEM images and particle size analysis. (C) Zeta potentials of ZnO NPs, ES, and ZnO@DE in aqueous solution. (D) XRD peak patterns. (E) XPS spectra of Cu2p and Zn2p in ZnO@DE. (F)The UV absorption peak of ES and ZnO@DE.

The XPS results indicate that the Cu2p peak is at 932.52 eV, while the Zn2p peak is at 1021.47 eV. We tested the characteristic UV absorption peaks of ES and ZnO@DE with the intensity of the characteristic UV absorption peak at 260 nm (Fig. 1E). These analyses revealed an encapsulation efficiency of 86.1% and a drug loading of 12.4% for ES.

Design of DNAzyme in ZnO@DE

The DNAzyme we designed targets ATP7B, a key protein responsible for copper excretion that maintains copper homeostasis and reduces cuproptosis. Studies have also shown the importance of the ATP7B gene in ovarian cancer development.[18] The downregulation of ATP7B leads to intracellular copper ion accumulation, thereby enhancing the cuproptosis response. First, we examined the expression of ATP7B under different nanoparticle interventions (Fig. 2A). ZnO NPs and ES had no significant effect. The cytotoxicity of these nanoparticles increased with concentration (Fig. 2B). Hemolysis testing indicated that ZnO@DE exhibited minimal toxicity toward red blood cells at low concentrations (Fig. 2C).

Next, we designed three different DNAzyme sequences targeting ATP7B and tested their cytotoxicity on SGC7901 cells (Fig. 2D). After treating gastric cancer cells with different ZnO@DE variants and analyzing ATP7B expression, we found that DNAzyme No. 3 exhibited significant ATP7B inhibition. We also proposed some application hypotheses, for example, Wilson's disease is a severe copper metabolism disorder caused by ATP7B gene mutation,[19,20] and whether these DNAzyme, which can regulate ATP7B, can be used as a therapeutic drug to increase the expression level of ATP7B. We constructed a DNAzyme, ZnO@DE (M), that only loaded non-functional sequences as the control group. After treatment of tumor cells with ZnO@DE (M), the expression level of ATP7B was significantly restored compared with that after treatment with ZnO@DE (Fig. 2E). Subsequently, we investigated the effect of DNAzyme No. 3 on ATP7B mRNA levels (Fig. 2F and G). In the presence of ZnO as a catalyst, DNAzyme significantly suppressed ATP7B mRNA expression.

Effects of ZnO@DE on intracellular signaling molecules

ZnO and ES play important roles in inducing ferroptosis[21] and cuproptosis.[22] We examined several markers involved in these cell death pathways under different treatments. Dihydrolipoamide Acetyltransferase (DLAT) is the core subunit of the pyruvate dehydrogenase complex (PDC) and contains lipoylation modifications. DLAT expression remained unchanged between the ZnO NPs and ZnO@DNAzyme groups, as well as between the ZnO NPs + ES and ZnO@DE groups, indicating that DNAzyme had no significant effect on DLAT expression, regardless of ES presence. However, DLAT expression was significantly inhibited when ZnO NPs and ES were combined (Fig. 3A). Heme Oxygenase 1 (HMOX1) is a key cellular stress response protein involved in iron metabolism and oxidative stress. DNAzyme significantly reduced HMOX1 expression in the ZnO NPs and ZnO@DNAzyme groups, suggesting that it may reduce ferroptosis (Fig. 3B). Glutathione peroxidase 4 (GPX4) is a crucial enzyme that eliminates lipid peroxides, particularly phospholipid peroxides (LPO),[23] protecting cells from oxidative stress. Protein expression analysis showed that DNAzyme did not significantly affect GPX4 expression, but

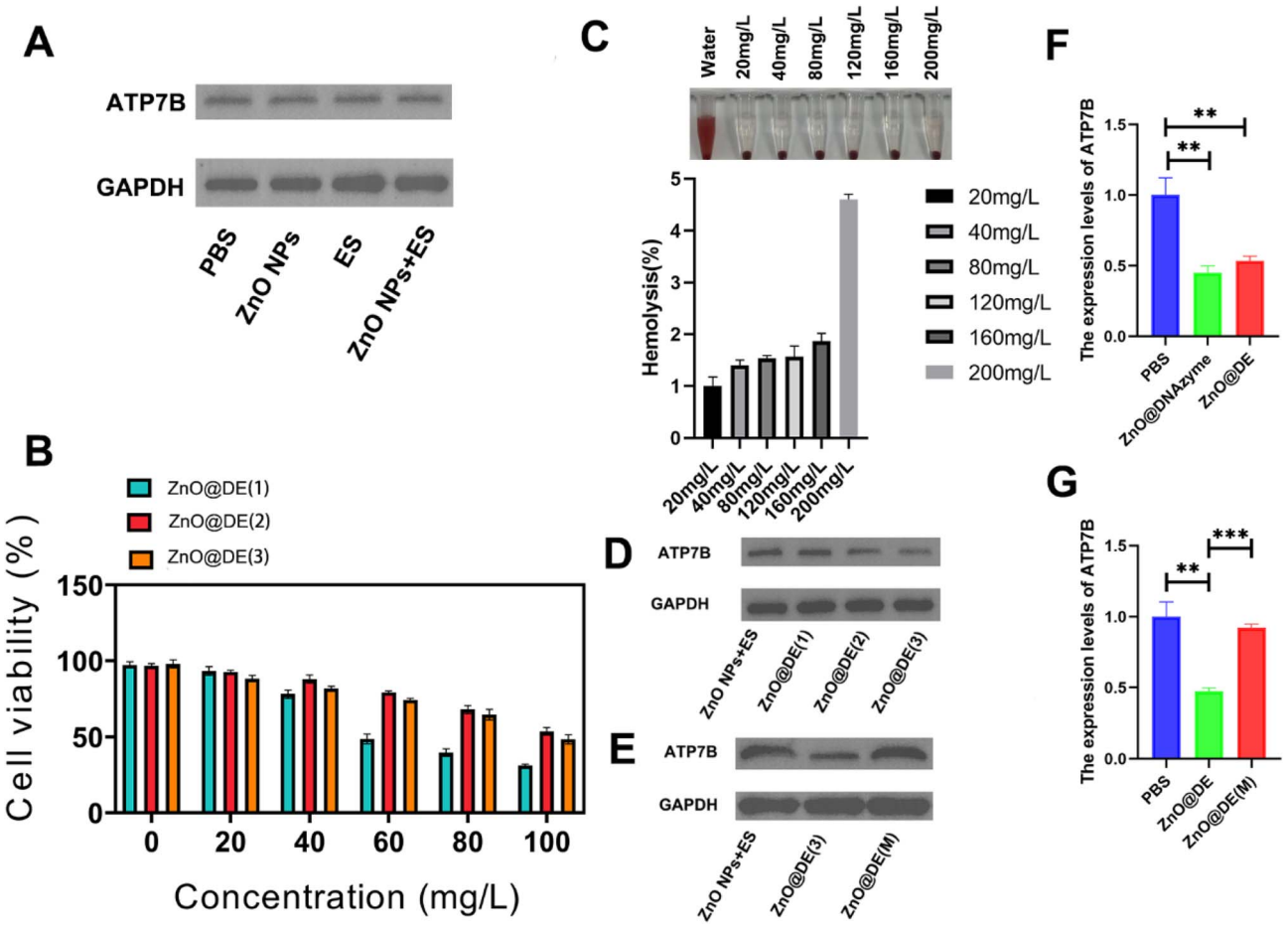

Fig. 2 Selection of DNAzyme. (A) ATP7B expression under ZnO NPs, ES, and ZnO NPs + ES treatment. (B) Cytotoxicity of different DNAzyme sequences in tumor cells. (C) Hemolysis test. (D and E) Inhibitory effects of different DNAzyme sequences on ATP7B protein expression. (F and G) Inhibitory effect of ZnO@DE and ZnO@DNAzyme on intracellular ATP7B mRNA.

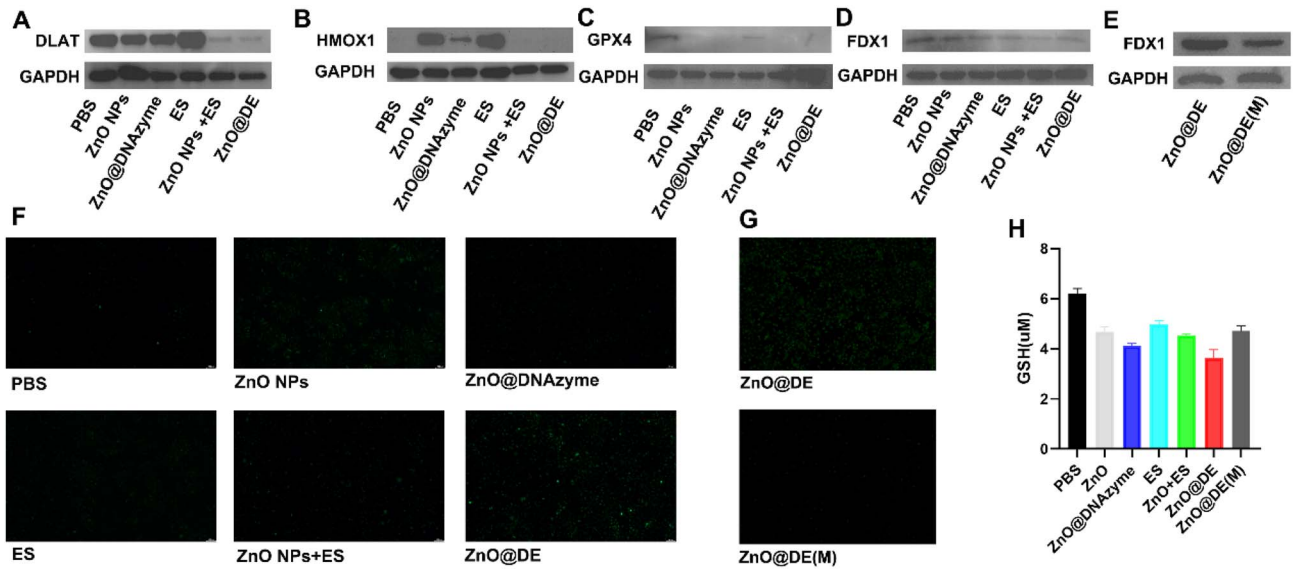

Fig. 3 Effects of ZnO@DE on intracellular signaling molecules. (A–E) Effects of ZnO NPs (80 mg L^{-1}), ZnO@DNAzyme (80 mg L^{-1}), ES (10 μM), ZnO NPs + ES, ZnO@DE (80 mg L^{-1}) and ZnO@DE(M) (80 mg L^{-1}) on the expression of DLAT, HMOX1, GPX4, and FDX1 proteins. (F–H) Effects of ZnO NPs, ZnO@DNAzyme, ES, ZnO NPs + ES, ZnO@DE and ZnO@DE(M) on intracellular ROS and GSH levels.

GPX4 levels were markedly suppressed upon ES addition (Fig. 3C). Ferredoxin 1 (FDX1) is a mitochondrial electron transfer protein that regulates copper-dependent protein acylation, Fe–S cluster synthesis, and steroid biosynthesis. In the presence of ES, DNAzyme significantly increased FDX1 expression, thereby promoting cuproptosis (Fig. 3D). After adding ZnO@DE (M), the expression level of FDX1 was significantly lower than that in the ZnO@DE group (Fig. 3E). We also measured intracellular ROS and GSH levels (Fig. 3F–H). The number of cell plates in each group was the same and the drug action time was short (2 hours), so fluorescence microscopy was used to observe the ROS. ZnO NPs significantly increased ROS levels, whereas ES alone had little effect. However, ZnO@DE induced the highest ROS production among all groups. GSH concentrations showed a general decreasing trend across different nanoparticle treatments, with ZnO@DE exhibiting the strongest GSH depletion effect.

Evaluation of ZnO@DE antitumor effects

The tumor-suppressive effect of nanoparticles is our primary concern. In a 12-hours *in vitro* wound healing assay, the addition of DNAzyme significantly reduced wound healing,

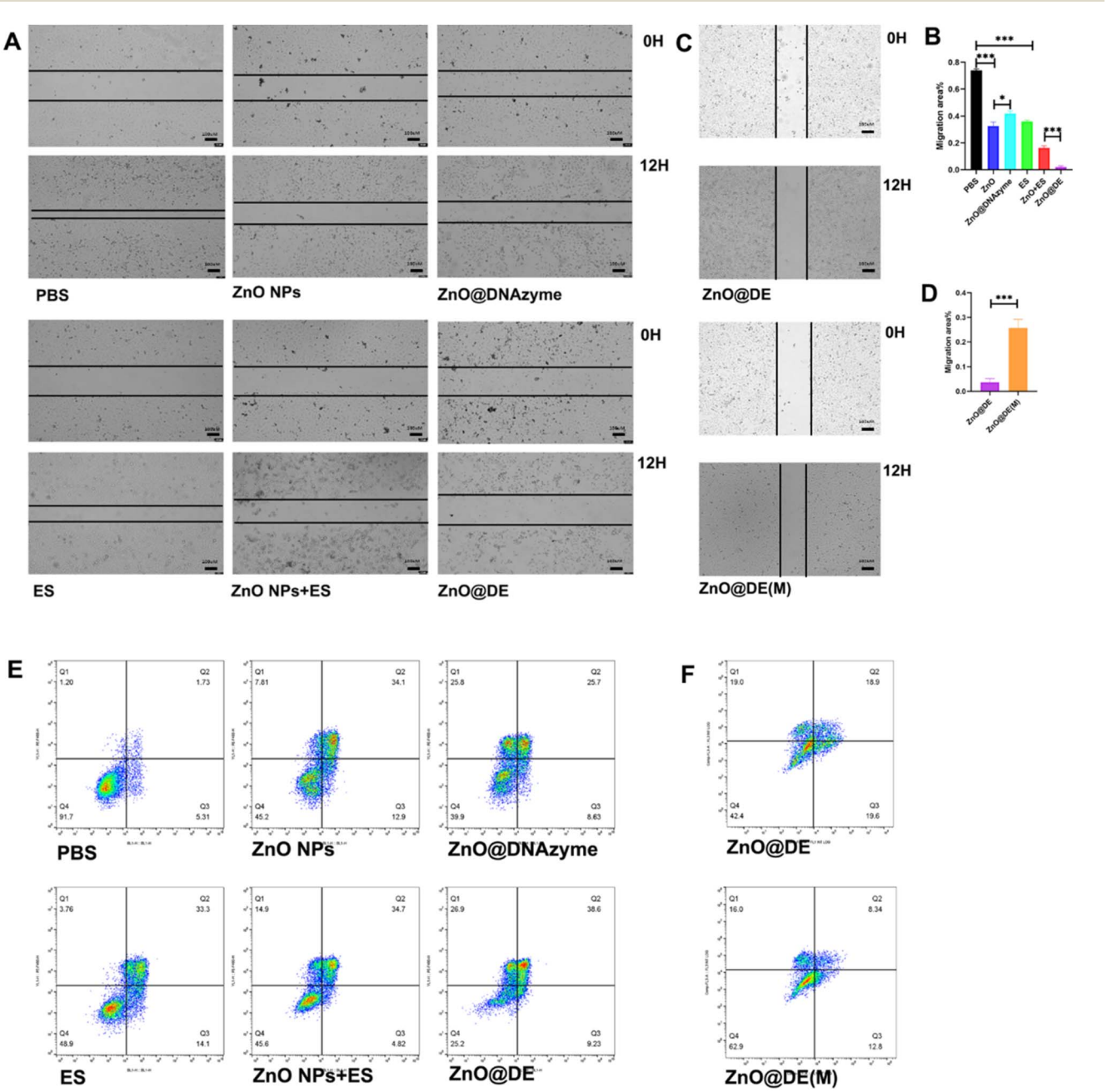

Fig. 4 *In vitro* validation of nanoparticle effects. (A–D) Wound healing assay showing the effects of ZnO NPs, ZnO@DNAzyme, ES, ZnO NPs + ES, ZnO@DE and ZnO@DE(M) on tumor cell invasion. (E and F) Flow cytometry analysis of apoptosis in tumor cells treated with ZnO NPs, ZnO@DNAzyme, ES, ZnO NPs + ES, ZnO@DE and ZnO@DE(M).

regardless of ES presence. The ZnO@DE group exhibited the most pronounced inhibition of wound healing (Fig. 4A–D). Observation of cell morphology revealed a significantly lower cell density in the ZnO@DE group after 12 hours of treatment, further impairing tumor cell migration. Flow cytometry was used to assess apoptosis among different treatment groups. The ZnO@DNAzyme group exhibited a significantly higher proportion of dead cells than the ZnO NPs group. In the presence of ES, DNAzyme further increased apoptosis, with the ZnO@DE group showing the most substantial apoptotic effect, demonstrating its superior tumor-killing potential (Fig. 4E and F).

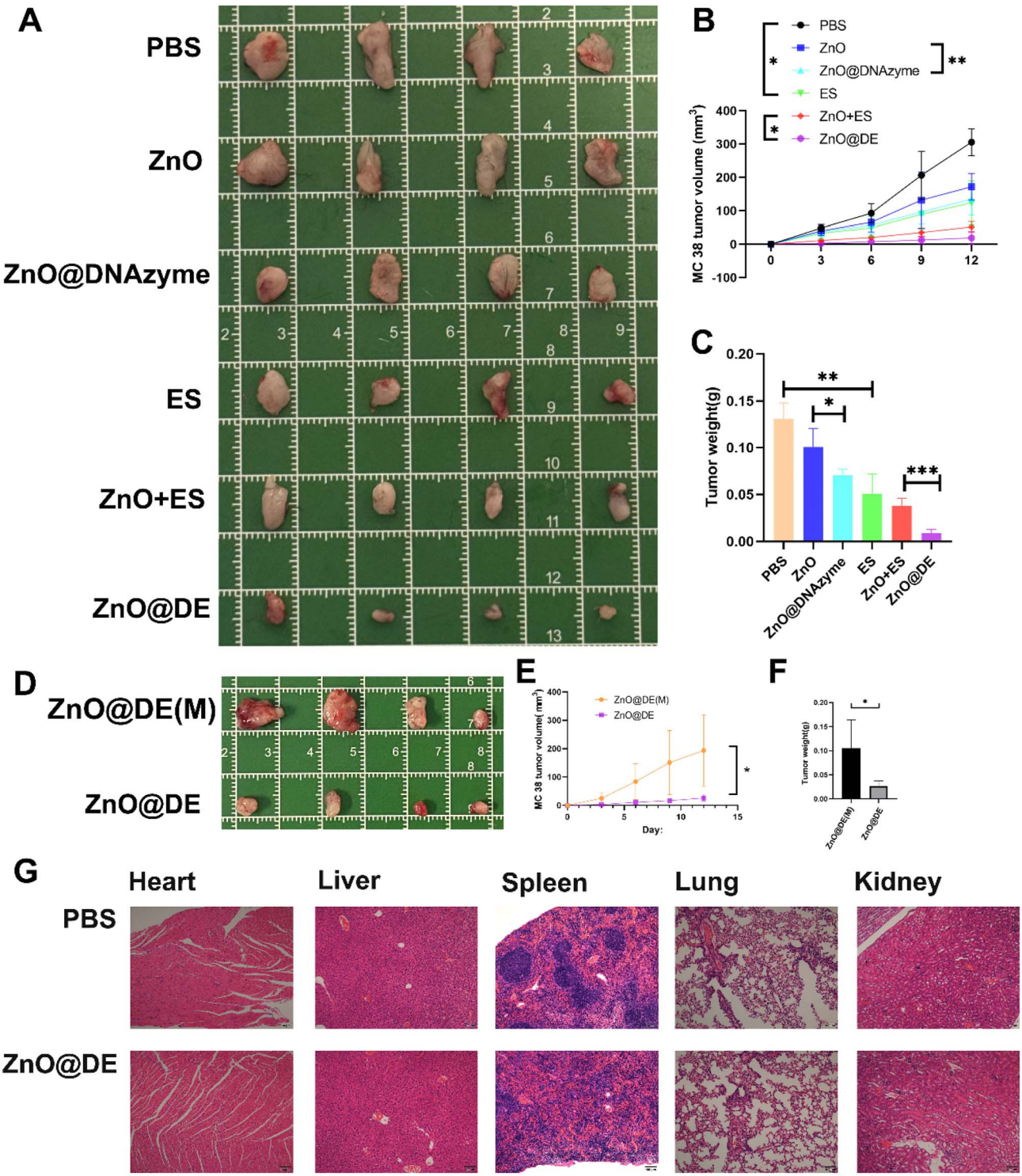

Fig. 5 *In Vivo* experimental validation. (A–F) Images, volume and weight comparisons of tumors excised from mice treated with PBS, ZnO NPs, ZnO@DNAzyme, ES, ZnO + ES, ZnO@DE and ZnO@DE(M). (G) The HE staining of heart, liver, spleen, lung, and kidney tissues.

In Vivo experimental validation

Our synthesized nanoparticles exhibited significant and effective anti-tumor activity *in vitro*. Next, we validated their anticancer effects *in vivo*. C57BL/6J mice with subcutaneously implanted MC38 gastric cancer cells were randomly divided into different groups (four mice per group). Each group received tail vein injections of PBS, ZnO NPs, ZnO@DNAzyme, ES, ZnO + ES or ZnO@DE (3 mg kg^{-1}) every three days. The results showed that ZnO alone had no significant effect on tumor size, whereas ES significantly inhibited tumor growth (Fig. 5A–C). Regardless of the presence of ES, gene silencing of ATP7B by DNAzyme led to a significant reduction in tumor size. Moreover, ZnO@ES demonstrated the most pronounced tumor inhibition effect, highlighting the superior anti-tumor efficacy of this combined nanoparticle system. Then we introduced an additional control group to compare with the tumors in the ZnO@DE group. It was found that the tumors in group ZnO@DE were significantly smaller in mass and volume than those in group ZnO@DE (M) (Fig. 5D–F). Additionally, HE staining of heart, liver, spleen, lung, and kidney tissues from mice in the ZnO@DE and PBS groups revealed no significant abnormalities in the ZnO@DE group (Fig. 5G).

Conclusion

Currently, inducing cuproptosis in tumor cells is considered a promising strategy in cancer therapy. One study synthesized a composite material composed of sandwich-type polyoxometalates, disulfide-bridged copper complexes, and hyaluronic acid, which could induce cuproptosis and, when combined with 808-nm near-infrared irradiation, greatly enhanced the inhibition of breast cancer cells.[24] Another study integrated a copper-based metal–organic framework (MOF) shell with loaded disulfiram (DSF) to activate cuproptosis and enhance cytotoxicity against breast cancer cells.[25] Additionally, chagosendine C was found to induce cuproptosis by targeting FDX1, increasing intracellular copper ions and ROS levels in colon cancer cells, ultimately leading to cell death.[26]

In summary, we developed a multifunctional nanoparticle platform, ZnO@DE, synthesized *via* a one-pot approach using ZnO NPs, DNAzyme, and ES. The unique physicochemical properties of this material suggest promising potential for healthcare applications. Given its high biocompatibility and efficient functional performance, this material may serve as a promising platform for drug delivery. This nanoparticle system demonstrated several advantages:[1] Programmability and Self-Assembly. By modifying the DNAzyme sequence, theoretically, any target gene-specific DNAzyme can be delivered into cells for gene silencing, making it a promising tool for diseases requiring target gene downregulation. ZnO NPs facilitate one-pot encapsulation, possess a well-defined structure, high loading capacity, and exhibit excellent biostability and biocompatibility.[2] Multifunctionality. ES induces cuproptosis, while DNAzyme-mediated ATP7B silencing further inhibits copper ion efflux. This disruption impairs potential tumor cell compensatory mechanisms against cuproptosis, thereby accelerating the process. However, this study also has some limitations. The cutting site and cutting efficiency of ATP7B by DNAzyme remain unclear. The in-depth exploration of the mechanism behind cuproptosis is still unclear. In terms of animal model selection, *in situ* models are more reliable. These are the issues we need to address in the next step. Overall, our newly developed nanoparticle platform and DNAzyme sequences can be easily adapted to other research directions, offering new insights into cancer therapy.

Ethics approval and consent to participate

All animal procedures were performed in accordance with the Guidelines for Care and Use of Laboratory Animals of Xiamen University and approved by the Animal Ethics Committee of Xiamen University.

Author contributions

HZ carried out the molecular genetic studies, drafted the manuscript, participated in the design of the study, performed the statistical analysis and conceived of the study. BD drafted the manuscript. QYK offer funding. All authors read and approved the final manuscript.

Conflicts of interest

The authors declare that they have no conflict of interest.

Data availability

The data supporting this article have been included as part of the supplementary information (SI). Supplementary information is available. See DOI: https://doi.org/10.1039/d5ra07735d.

References

1 L. Chen, J. Min and F. Wang, Copper homeostasis and cuproptosis in health and disease, *Signal Transduction Targeted Ther.*, 2022, 7(1), 378.
2 C. Zhang, T. Huang and L. Li, Targeting cuproptosis for cancer therapy: mechanistic insights and clinical perspectives, *J. Hematol. Oncol.*, 2024, **17**(1), 68.
3 L. M. Guthrie, S. Soma, S. Yuan, A. Silva, M. Zulkifli, T. C. Snavely, *et al.*, Elesclomol alleviates Menkes pathology and mortality by escorting Cu to cuproenzymes in mice, *Science*, 2020, **368**(6491), 620–625.
4 P. A. Lang, M. Schenck, J. P. Nicolay, J. U. Becker, D. S. Kempe, A. Lupescu, *et al.*, Liver cell death and anemia in Wilson disease involve acid sphingomyelinase and ceramide, *Nat. Med.*, 2007, **13**(2), 164–170.
5 E. Tokuda, Y. I. Takei, S. Ohara, N. Fujiwara, I. Hozumi and Y. Furukawa, Wild-type Cu/Zn-superoxide dismutase is misfolded in cerebrospinal fluid of sporadic amyotrophic lateral sclerosis, *Mol. Neurodegener.*, 2019, **14**(1), 42.

6 S. Lutsenko, S. Roy and P. Tsvetkov, Mammalian copper homeostasis: physiological roles and molecular mechanisms, *Physiol. Rev.*, 2025, **105**(1), 441–491.
7 S. Wang, Y. Liu, M. Su, Y. Wang, W. Wang, W. Wang, *et al.*, Near-Infrared Activatable Copper Nanoplatforms Synergize with the 5-Azacytidine Prodrug to Potentiate Cuproptosis, *Angew Chem. Int. Ed. Engl.*, 2024, **63**(52), e202411609.
8 Z. Z. Li, L. Guo, Y. L. An, W. J. Yu, D. Y. Shi, Q. Y. Lin, *et al.*, Evolocumab attenuates myocardial ischemia/reperfusion injury by blocking PCSK9/LIAS-mediated cuproptosis of cardiomyocytes, *Basic Res. Cardiol.*, 2025, 301–320.
9 N. Wang, Y. Liu, D. Peng, Q. Zhang, Z. Zhang, L. Xu, *et al.*, Copper-Based Composites Nanoparticles Improve Triple-Negative Breast Cancer Treatment with Induction of Apoptosis-Cuproptosis and Immune Activation, *Adv. Healthcare Mater.*, 2024, **13**(28), e2401646.
10 Z. Chen, J. Wang, Y. Ruan, J. Cao, H. Jiang, J. Jiang, *et al.*, Diatomic Mn/Ca Nanozymes with Jaw Vascular Unit Mimicry for Triple-Enzyme Synergistic Therapy of Osteoradionecrosis, *Adv. Mater.*, 2025, e17968.
11 H. Gao, J. Luo, X. Chen, Y. Huang, M. Mo, Q. Luo, *et al.*, Immunomodulatory copper-based polyphenol nanozyme for diabetic infectious wound healing *via* NIR amplified cuproptosis bacteriostat in synergy with ferroptosis inhibition anti-inflammation, *Bioact. Mater.*, 2025, **54**, 759–776.
12 M. Zhang, H. Zheng, H. Jin, X. Zhu, S. Liu, Y. Chen, *et al.*, Regulating SLC7A11/GSH/GPX4 axis by glucose dyshomeostasis to simultaneously promote disulfidptosis, cuproptosis and ferroptosis, *Bioact. Mater.*, 2025, **54**, 744–758.
13 J. Yan, M. Ran, X. Shen and H. Zhang, Therapeutic DNAzymes: From Structure Design to Clinical Applications, *Adv. Mater.*, 2023, **35**(30), e2300374.
14 S. Ekesan and D. M. York, Dynamical ensemble of the active state and transition state mimic for the RNA-cleaving 8-17 DNAzyme in solution, *Nucleic Acids Res.*, 2019, **47**(19), 10282–10295.
15 Y. Wang, K. Nguyen, R. C. Spitale and J. C. Chaput, A biologically stable DNAzyme that efficiently silences gene expression in cells, *Nat. Chem.*, 2021, **13**(4), 319–326.
16 S. Zhi, X. Zhang, J. Zhang, X. Y. Wang and S. Bi, Functional Nucleic Acids-Engineered Bio-Barcode Nanoplatforms for Targeted Synergistic Therapy of Multidrug-Resistant Cancer, *ACS Nano*, 2023, **17**(14), 13533–13544.
17 R. Jiang, L. Li and M. Li, Biomimetic Construction of Degradable DNAzyme-Loaded Nanocapsules for Self-Sufficient Gene Therapy of Pulmonary Metastatic Breast Cancer, *ACS Nano*, 2023, **17**(21), 22129–22144.
18 K. Tecza, J. Pamula-Pilat, Z. Kolosza, N. Radlak and E. Grzybowska, Genetic polymorphisms and gene-dosage effect in ovarian cancer risk and response to paclitaxel/cisplatin chemotherapy, *J. Exp. Clin. Cancer Res.*, 2015, **34**(1), 2.
19 D. Huster, A. Kuhne, A. Bhattacharjee, L. Raines, V. Jantsch, J. Noe, *et al.*, Diverse functional properties of Wilson disease ATP7B variants, *Gastroenterology*, 2012, **142**(4), 947–56e5.
20 H. Cai, X. Cheng and X. P. Wang, ATP7B gene therapy of autologous reprogrammed hepatocytes alleviates copper accumulation in a mouse model of Wilson's disease, *Hepatology*, 2022, **76**(4), 1046–1057.
21 B. Tian, R. Tian, S. Liu, Y. Wang, S. Gai, Y. Xie, *et al.*, Doping Engineering to Modulate Lattice and Electronic Structure for Enhanced Piezocatalytic Therapy and Ferroptosis, *Adv. Mater.*, 2023, **35**(38), e2304262.
22 B. Guo, F. Yang, L. Zhang, Q. Zhao, W. Wang, L. Yin, *et al.*, Cuproptosis Induced by ROS Responsive Nanoparticles with Elesclomol and Copper Combined with alphaPD-L1 for Enhanced Cancer Immunotherapy, *Adv. Mater.*, 2023, **35**(22), e2212267.
23 J. Xu, G. Guan, Z. Ye, C. Zhang, Y. Guo, Y. Ma, *et al.*, Enhancing lipid peroxidation *via* radical chain transfer reaction for MRI guided and effective cancer therapy in mice, *Sci. Bull.*, 2024, **69**(5), 636–647.
24 M. Zhang, S. Yang, M. Liu, Y. Chen, Q. Dou, R. Jia, *et al.*, Tungstotellurate(VI)-Based Nanocomposite Inhibits Breast Cancer Proliferation and Metastasis by Enhancing Cuproptosis and Apoptosis, *Angew Chem. Int. Ed. Engl.*, 2025, e202514795.
25 Y. Tang, L. Ge, D. Zhu, R. Hu, W. Chen, X. Zhen, *et al.*, A Tumor Microenvironment-Responsive Self-Oxygenating Nanoplatform for Dual-Enhanced Cuproptosis and Sonodynamic Synergistic Immunotherapy, *ACS Nano*, 2025, **19**(45), 39228–39240.
26 X. Tao, H. Wang, Q. Wang, C. Wang, C. W. Shao, Y. Jin, *et al.*, Marine Natural Product Chagosendine C Induces Cuproptosis in Colorectal Cancer Cells by Targeting FDX1, *J. Am. Chem. Soc.*, 2025, **147**(41), 37089–37103.